

# RETRACTED ARTICLE: PVT1 Promotes the Proliferation and Migration of Non-Small Cell Lung Cancer via Regulating miR-148/RAB34 Signal Axis

This article was published in the following Dove Press journal:  
*OncoTargets and Therapy*

Yong Xi<sup>1,\*</sup>  
Weiyu Shen<sup>1,\*</sup>  
Chenghua Jin<sup>1</sup>  
Lijie Wang<sup>1</sup>  
Bengtong Yu<sup>1,2</sup>

<sup>1</sup>Department of Thoracic Surgery, Ningbo Medical Center Lihuili Eastern Hospital, Ningbo, Zhejiang 315040, People's Republic of China; <sup>2</sup>Department of Thoracic Surgery, The First Affiliated Hospital of Nanchang University, Nanchang, Jiangxi 330006, People's Republic of China

\*These authors contributed equally to this work

**Objective:** It has been verified that long non-coding RNAs (lncRNAs) play critical roles in the development of human cancers. Increasing evidence indicates that lncRNA human plasmacytoma variant translocation1 (PVT1) was up-regulated in non-small cell lung cancer (NSCLC) which is the leading cause of cancer-related death. However, the precise mechanism underlying the effect of PVT1 remains elusive. Our research focused on the correlation of PVT1 to miR-148 and RAB34 in NSCLC.

**Methods:** The quantitative real-time PCR (qRT-PCR) and western blot assay were used to detect gene and protein expression in NSCLC tissues and cells. CCK8, colony formation, transwell and wound healing assays were performed to evaluate the cell function of NSCLC cells. Dual-luciferase activity assay and RNA pull down assays were performed to verify the interaction between miR-148 and its targets. A xenograft test was conducted to detect the impact of RAB34 on tumor development in vitro.

**Results:** In NSCLC tissues and cells, PVT1 and RAB34 were up-regulated, and miR-148 was down-regulated. Overexpression of PVT1 was capable of promoting NSCLC cell proliferation and migration which could be reversed by miR-148 restoration or RAB34 knockdown. Also, our data firstly determined that the down-regulation of RAB34 had inhibitory effects while the up-regulation of RAB34 had promotive effects on tumor growth in vitro and in vivo.

**Conclusion:** Those findings indicated that the signal pathway PVT1/miR-148/RAB34 play critical roles in the progression of NSCLC could be proposed in NSCLC as a possible diagnosis or therapeutic targets.

**Keywords:** NSCLC, RAB34, PVT1, miR-148, proliferation, migration

## Introduction

Long non-coding RNAs (lncRNAs) are a novel group of ncRNAs with the length of more than 200 nucleotides.<sup>3</sup> lncRNAs are capable of regulating gene expression at epigenetic, transcriptional and post-transcriptional levels, thus, participating in various of pathological process such as autophagy, necrosis and apoptosis.<sup>4-6</sup> lncRNAs have been confirmed to play vital roles in cancer progression, metastasis, prognosis and drug resistance in NSCLC.<sup>7</sup> lncRNA human plasmacytoma variant translocation1 (PVT1) as a novel potential biomarker for diagnosis and prognosis of NSCLC inhibited the expression of p15 and p21.<sup>8</sup> PVT1 also acts as a competing endogenous RNA for miR-497 which can promote the progression of NSCLC.<sup>9</sup> Wan et al have done in-depth research and proved that PVT1 promoted the

Correspondence: Bengtong Yu  
Department of Thoracic Surgery, The First Affiliated Hospital of Nanchang University, Nanchang, Jiangxi 330006, People's Republic of China  
Email hmBengtongYu@outlook.com

proliferation of NSCLC cells via regulating LATS2 expression.<sup>10</sup> Moreover, a previous study revealed that knockdown of PVT1 improved NSCLC radiosensitivity by sponging miR-195.<sup>11</sup> Further research has demonstrated that PVT1 could function as an endogenous competing RNA for miR-216b to inhibit NSCLC cisplatin sensitivity.<sup>12</sup>

MiR-148/152 was shown in prior studies to be a prospective biomarker in NSCLC.<sup>13</sup> The plasma expression levels of miR-148/152 may be useful biomarkers for the early diagnosis of NSCLC in NSCLC patients.<sup>14</sup> RAB family proteins are small GTPases engaged in the transport of proteins. RAB34 is belonging to the RAB family that are associated with many cancers.<sup>15</sup> A tumor suppressor-folliculin directs the formation of Rab34–RILP complex to regulate the nutrient-dependent dynamic distribution of lysosomes.<sup>16</sup> A previous study showed that RAB34 targeted miR-9 was up-regulated in human gastric carcinoma.<sup>17</sup> RAB34 can also control breast cancer cell adhesion, migration, and invasion.<sup>15</sup> In addition, RAB34 expression was linked with the progression of glioma grade and conferred as a prognosis-associated biomarker in gliomas.<sup>18</sup>

In our research, the correlation between PVT1 and miR-148 and RAB34 in NSCLC was investigated. We have demonstrated that PVT1 promotes NSCLC cell proliferation and migration and then find that miR-148 directly targets PVT1. Also, RAB34 was confirmed as a direct target of miR-148. We discovered that PVT1 and RAB34 were up-regulated and miR-148 was down-regulated in tissues and cells of NSCLC. RAB34, regulated by PVT1 and miR-148, promoted the in vivo and in vitro proliferation and migration of the NSCLC cells. In short, the signal pathway PVT1/miR-148/RAB34 may serve as a promising therapeutic target for NSCLC.

## Materials and Methods

### Clinical Tissues Collection

We collected 25 paired NSCLC and adjacent normal lung tissues from patients at Ningbo Medical Center Lihuili Eastern Hospital. These patients were diagnosed with NSCLC and did not receive radiotherapy or chemotherapy prior to surgery. The tissues were stored in liquid nitrogen and transferred to laboratory. The written informed consent was obtained from all patients with NSCLC. The study including the xenograft assay was approved by the Ethics Committee of the Ningbo Medical Center Lihuili

Eastern Hospital and was conducted in accordance with the Declaration of Helsinki.

### Cell Culture

The human normal bronchial epithelial cell line NHBE and NSCLC cell lines (A549, H1299, SPCA1, H2279, H1975, H1650, HC827) were purchased from American Type Culture Collection (ATCC, USA). A549 and H1299 cells were cultured in RPMI-1640 medium (GIBCO, NY, USA) and other cells (SPCA1, H2279, H1975, H1650, HC827) were cultured in DMEM medium supplemented with 10% fetal bovine serum, penicillin (100 U/mL) and streptomycin (100 mg/mL). All cells were maintained in an environment of 37°C and 5% CO<sub>2</sub>.

### Quantitative Reverse Transcription PCR (qRT-PCR)

For qRT-PCR analysis, total RNA was extracted using TRIzol reagent (Invitrogen, CA, USA) and were reverse transcribed into cDNA using PrimeScript RT reagent Kit (TaKaRa, Dalian, China) according to the manufacturer's instructions. The SYBR® Premix Ex Taq™ (TaKaRa, Dalian, China) was used to perform quantitative RT-PCR in a 20 µl reaction which was subsequently proceeded in a Real-Time PCR detection system (Applied Biosystems™, USA). The qRT-PCR analysis of miRNA was performed using the All-in-One™ miRNA qRT-PCR detection kit (Genecopeia, MD, USA). The  $\Delta\Delta C_t$  was calculated by subtracting the  $\Delta C_t$  of the control cells from the  $\Delta C_t$  of the experimental cells. Fold change was generated using the  $2^{-\Delta\Delta C_t}$  equation. The qRT-PCR primer sequences used are as follows:

miR-148-forward: 5' TGCGGTCAGTGCCTACAGAA C3'; miR-148-forward: 5' CCAGTGCAGGGTCCGAGGT 3';  
PVT1-forward: 5' CTTTCAGCACTCTGGACGGACT TG 3';  
PVT1-reverse: 5' GATCTATGGCATGGGCAGGGT AG 3';  
RAB34-forward: 5' TGCACGGGCACAAAGACTTC CAC 3';  
RAB34-reverse: 5' CCCAGCACCTCAAATCGTTCC AT 3';

### Cell Transfection

The pcDNA3.1-PVT1 vector was synthesized by General Biosystems (Anhui, China). MiR-148 mimics, miR-148 inhibitor and their corresponding negative control were also

purchased from General Biosystems. The shRNA of RAB34 was designed and synthesized by Sigma (St. Louis, MO, USA). Transfections were carried out using Lipofectamine 3000 reagent (Thermo Fisher Scientific, CA, USA) according to the manufacturer's instructions.

### Cell Viability Assay

After 24hrs of transfection, A549 and H1299 cells were seeded onto 96-well plates (1000 cells/well). The cell viability assay was conducted by CCK8 according to the manufacturer's protocol. The original medium was removed and replaced with culture medium containing 10% CCK8 at 12, 24, 48, 72 hrs after cells were seeded. 4hrs after incubation, the absorbance at 450nm was measured using a microplate reader (Bio-Rad, CA, USA). Each test was performed in triplicate.

### Colony Formation Assay

500 A549 and H1299 cells after transfection were seeded onto 12-well plates. After 14 days of incubation, the cells were fixed with 4% paraformaldehyde for 15 mins and stained with 0.1% crystal violet for 30mins. The clones were photographed with a microscope (Leica, Germany). The number of visible clones indicated the ability of cell clone formation. The assay was conducted for three independent times.

### Transwell Assay

1×10<sup>5</sup> cells were seeded onto the upper chamber of each 24-well plate (Corning, NY, USA) with serum-free medium. The pore size of the upper chamber was 8.0 µm. The lower chamber was filled with 600 µL of medium containing 10% FBS. After incubation for 24 hrs, the cells attached to the reverse phase of the membrane were fixed with 4% paraformaldehyde for 15 min and the cells on the upper chamber were removed using cotton swabs. Then, the cells attached on the lower surface were stained with 0.1% crystal violet for 5 min. Cells were photographed for at least five fields using a light microscope (Leica, Germany).

### Wound Healing Assay

The transfected cells were seeded onto 24-well plates (1×10<sup>5</sup> cells/well). The seeded cells were cultured overnight and a scratch was introduced with a pipette tip. Then the cells were washed with PBS for three times. At 0h and 48h, the images were captured under a light microscope. The scratch area was calculated by ImageJ software. At

least five fields of each group were evaluated. The value of relative migration distance (%) is obtained through dividing the scratch area at 48hrs by that at 0hrs.

### Dual-Luciferase Reporter Assay

The binding sites between miR-148 and RAB34 or miR-148 and PVT1 were predicted by bioinformatics analysis tool TargetScan (<http://www.starbase.sysu.edu.cn>). The predicted binding sequence or mutant binding sites of PVT1 and RAB34 were synthesized by General Biosystems and cloned into pGL3 vector (Promega, Madison, USA) vector. Wild type or mutant type of luciferase reporter plasmid was co-transfected with miR-148 mimic or mimic control in A549 and H1299 cells using Lipofectamine 3000 (Thermo Fisher Scientific) according to the manufacturer's protocols. After 48 h, the lysed cells were exploited for luciferase activities analysis using a Dual-Luciferase Assay kit (GeneCopoeia, MD, USA).

### RNA Pull-Down Assay

A549 and H1299 cells were transfected with biotinylated probe such as biotin-miR-148 or biotin-NC. We collected the cells after 48hrs. The cells were lysed by specific lysis buffer for 10mins. M-280 streptavidin beads (Sigma, CA, USA) pre-coated with BSA and yeast tRNA were used to incubate with the lysate at 4°C for 4hrs. Then, the beads were washed with pre-cooled lysis buffer for three times, washed with low salt buffer for three times and then high salt buffer for two times. Finally, we performed qRT-PCR to detect the enrichment of lncRNA PVT1.

### Western Blot

The cells were collected and lysed in ice-cold RIPA lysis buffer (Thermo Fisher Scientific, CA, USA). The protein was quantified with the BCA kit (TaKaRa, Dalian, China). A total of 40ug protein was separated by 10% (SDS)-polyacrylamide gel for electrophoresis and then transferred onto polyvinylidene difluoride (PVDF) membrane. The 1× Tris-buffered saline with Tween (TBST) containing 5% nonfat milk was used to block the non-specific staining for 1 hr at room temperature. The membranes were then incubated with specific primary antibodies against RAB34 (Abcam, 1:1000) and GAPDH (Abcam, 1:3000) at a temperature of 4°C overnight. The 2 h of incubation was conducted at room temperature with the corresponding secondary antibodies (Abcam, 1:10,000). The bands were visualized with an ECL kit (Pierce, USA) in a darkroom and

analyze the gray scale of the strip by lab V 2.01 image analysis software (Total Lab, England).

## Immunohistochemistry

6 pairs of paraffin-embedded non-small cell lung cancer tumor and the adjacent normal tissues were sectioned and de-waxed conventionally. Antigen retrieval was done by microwave heating for three times and added with antigen retrieval buffer containing citrate buffer. Sections were incorporated with 0.5% hydrogen peroxide acting as the blocking buffer for 20 min at room temperature to block endogenous peroxidase activity. Then, the slides were incubated with specific primary antibody of RAB34 (1:300, abcam, England) at a temperature of 4°C overnight followed by incubating with the secondary antibody for 2 h at room temperature. Immunostaining was performed using DAB according to the manufacturer's instructions. The protein expression of RAB34 was observed under a microscope. The integrated optical density (IOD value) of three randomly selected fields from each slide was analyzed using Image ProPlus 6.0 software.

## Nude Mice Xenograft Assay

A total of 20 Male BALB/c nude mice (4–6 weeks old, 18–22 g) were purchased by Vital River Laboratory Animal Technology Company (Beijing, China) and randomly divided into four groups (pcDNA3.1-RAB34, pcDNA3.1, sh-RAB34 and sh-NC, N = 5/group). The mice were housed in a specific pathogen-free environment with a temperature of 25°C and 60% relative humidity.  $5 \times 10^6$  transferred A549 cells were suspended in 100 µl PBS and inoculated subcutaneously into the dorsal flanks of nude mice. Tumor growth was monitored every 2 days after the tumor appeared and the volume was calculated by the following equation: tumor volume =  $1/2 \times (\text{width})^2 \times \text{length}$ . The mice were killed and the tumors were weighed after 23 days of cell inoculation. All the animal procedures were performed in accordance with the guidelines of Ningbo Medical Center Lihuli Eastern Hospital Animal Care and Use Committee.

## Statistical Analysis

The date statistical significance analysis was performed using Prism GraphPad5.0 and SPSS 20.0 software. Student *t*-test was used to compare between two different groups while one-way ANOVA was used to evaluate the difference among multiple groups.  $p < 0.05$  was considered to be statistically significant.

## Results

### The Expression of PVT1 Is Up-Regulated in NSCLC and Associated with Poor Prognosis

Previous study revealed that PVT1 was up-regulated in NSCLC.<sup>16</sup> To verify this result and lay the foundation for further experiments, we found that PVT1 was up-regulated in NSCLC tissues compared with normal lung tissues via analyzing the profiles of NSCLC patient from Gene Expression Omnibus (GEO) dataset (Figure 1A). Then, 25 paired NSCLC tissue and matched normal tissues were collected and the expression of PVT1 was evaluated by qRT-PCR. The results also revealed an elevation of PVT1 level in NSCLC tissues (Figure 1B). The qRT-PCR results showed that the expression level of PVT1 was elevated at different degrees compared to the NHBE group, with PVT1 at highest level in A549 in NSCLC cell lines including A549, A1299, SPCA1, H2279, H1975, H1650 and HC827 (Figure 1C). The additional findings from KM plotter dataset showed that patients with greater PVT1 had shorter survival times while patients with reduced PVT1 had a longer survival time (Figure 1D). This finding was highly indicated PVT1 as a prognostic predictor of NSCLC.

### Cell Proliferation and Migration Were Promoted by Over-Expression of PVT1 in NSCLC Cells

To investigate the effect of PVT1 on NSCLC cell proliferation and migration, we selected A549 and H1299 cell lines. The over-expression of pcDNA3.1-PVT1 and corresponding negative control (pcDNA3.1) were transfected into A549 and H1299 cells. The efficiency of transfection was verified by qRT-PCR analysis (Figure 2A). The effect of PVT1 on cell proliferation was demonstrated by CCK8 assay and clone formation assay. CCK8 assay revealed that PVT1 over-expression promoted the cells viability in A549 and H1299 (Figure 2B). The clone formation assay showed that overexpression of PVT1 in A549 and H1299 cells promoted the proliferative capacity compared with the control group (Figure 2C). The transwell assay and wound healing assay revealed that the A549 and H1299 cells migration were accelerated by the transfection of pcDNA3.1-PVT1 vector (Figure 2D and E). In summary, the results showed that PVT1 promoted NSCLC cells proliferation and migration.



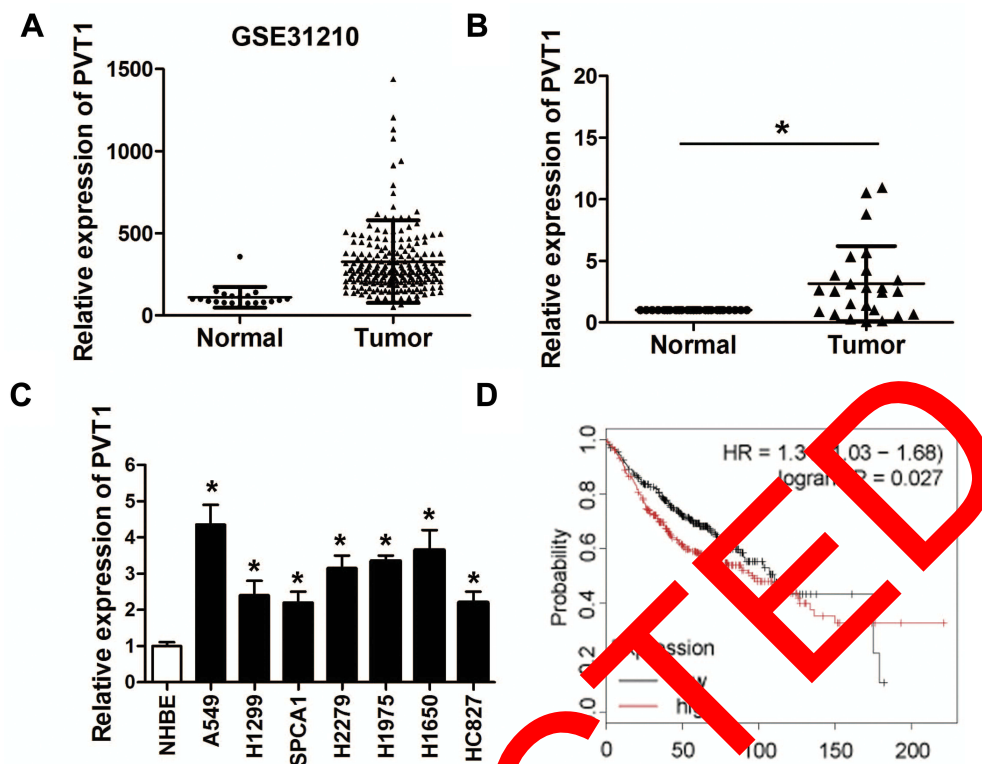


**Figure 1** LncRNA PVT1 expression is up-regulated in NSCLC and correlated with poor prognosis of patients with NSCLC. **(A)** Relative expression of PVT1 in the profiles of NSCLC patient tissues from GEO. **(B)** PVT1 expression in 25 paired NSCLC tissues compared with normal tissues was detected by qRT-PCR assay. **(C)** PVT1 expression was examined by qRT-PCR in NSCLC cell lines (A549, H1299, SPCA1, H2279, H1975, H1650, HC827) and human normal bronchial epithelial cell line (NHBE). **(D)** Up-regulation of PVT1 expression is associated with poor prognosis. Kaplan-Meier survival of NSCLC patients on PVT1 high- and low-expression groups was analyzed by KM plotter software. \* $p < 0.05$  vs normal or NHBE group.

Cell proliferation and migration were inhibited by knock down of PVT1 in NSCLC cells.

To further verify the effect of PVT1 on NSCLC cell proliferation and migration, lnc siRNA knocking down PVT1 and the negative control was transfected into A549 and H1299 cells. The efficiency of transfection was verified by qRT-PCR analysis (Figure 3A). CCK8 and clone formation assay revealed that PVT1 knock down inhibited the cell viability and proliferative capacity in A549 and H1299 (Figure 3B and C). The transwell assay and wound healing assay revealed that the A549 and H1299 cells migration was inhibited by knockdown of PVT1 (Figure 3D and E). In summary, the results showed that PVT1 knockdown inhibited NSCLC cells proliferation and migration.

## MiR-148 Is a Direct Target of PVT1 and Is Down-Regulated in NSCLC

To explicate the mechanisms underlying effects of PVT1 in NSCLC, we conducted bioinformatics analysis to search the targets of PVT1 with the help of TargetScan database. We cloned the wild and mutant sequence predicted as the

binding site in the 3'UTR of PVT1 (Figure 4A). The luciferase reporter assay showed that the co-transfection of miR-148 mimics largely decreased the activity of the reporter plasmid containing PVT1-wt but not PVT1-mut (Figure 4B). The effect of miR-148 on the expression of PVT1 was performed by qRT-PCR. As expected, the results suggested that over-expression of miR-148 inhibited the expression level of PVT1, inversely, inhibition of miR-148 promoted the expression of PVT1 (Figure 4C). Furthermore, RNA pull-down assay demonstrated that PVT1 was co-precipitated with miR-148, revealing that miR-148 can bind to PVT1 (Figure 4D).

We next investigated the expression and effect of miR-148 in NSCLC. First, qRT-PCR was performed to evaluate the expression of miR-148 in various NSCLC cell lines. The results showed that NSCLC cell lines (A549, H1299, SPCA1, H2279, H1975, H1650, HC827) expressed lower levels of miR-148 compared with the normal bronchial epithelial cell line (NHBE) (Figure 4E). Next, we checked the expression of miR-148 in 25 paired of NSCLC tissue and matched normal tissues by qRT-PCR. The expression of miR-148 was significantly reduced in NSCLC tissues

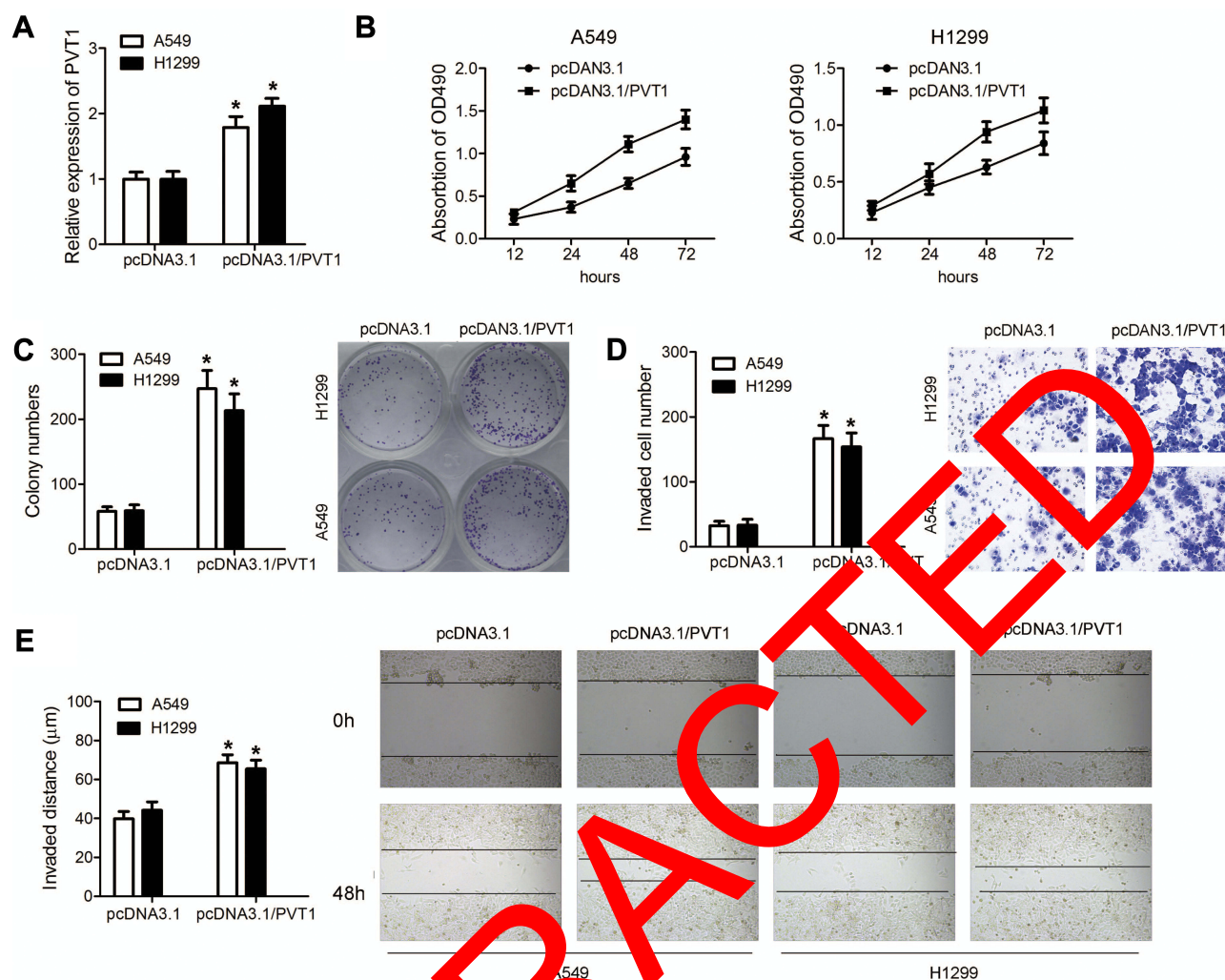


**Figure 2** PVT1 promotes the proliferation and migration of NSCLC cell lines in vitro. **(A)** Transfection effect of PVT1 was detected by qRT-PCR assay. **(B)** Proliferation ability of each group was measured by CCK-8 assay and **(C)** colony formation assay. **(D)** Migration ability of each group was detected by transwell assay and **(E)** wound healing assay. \* $p < 0.05$  vs pcDNA3.1 group.

compared with control (Figure 4F). Furthermore, we conducted a Kaplan–Meier survival analysis to find that patients with lower miR-148 levels exhibited a shorter survival time (Figure 4G). Finally, we analyzed the correlation between PVT1 and miR-148 expression in NSCLC tissues, suggesting that there was a significantly negative correlation between them (Figure 4H).

## MiR-148 Reversed the Effect of PVT1 in NSCLC

In order to verify the relationship between miR-148 and PVT1, rescue experiment was carried out. Over-expressing vector of PVT1 and miR-184 mimic was co-transfected into A549 and H1299 cells. CCK8 assay revealed that the co-transfection of PVT1 over-expressing vector and miR-148 mimic reduced the cells' viability in A549 and H1299 cells

compare to the PVT1 over-expression group (Figure 5A). Clone formation assay also showed that miR-148 reduced the number of colonies in comparison with PVT1 group (Figure 5B). Similarly, transwell assay and wound healing assay both revealed that miR-148 reversed the migration of A549 and H1299 cells compare to PVT1 group (Figure 5C and D).

## RAB34 Is a Direct Target of miR-148 and Up-Regulated in NSCLC

Furthermore, we predicted the putative binding sites of miR-148 and RAB34 using TargetScan website and designed 3'UTR mutant of RAB34 for luciferase reporter assay (Figure 6A). The luciferase reporter assay revealed that miR-148 mimics markedly suppressed the luciferase activity of the reporter plasmid containing

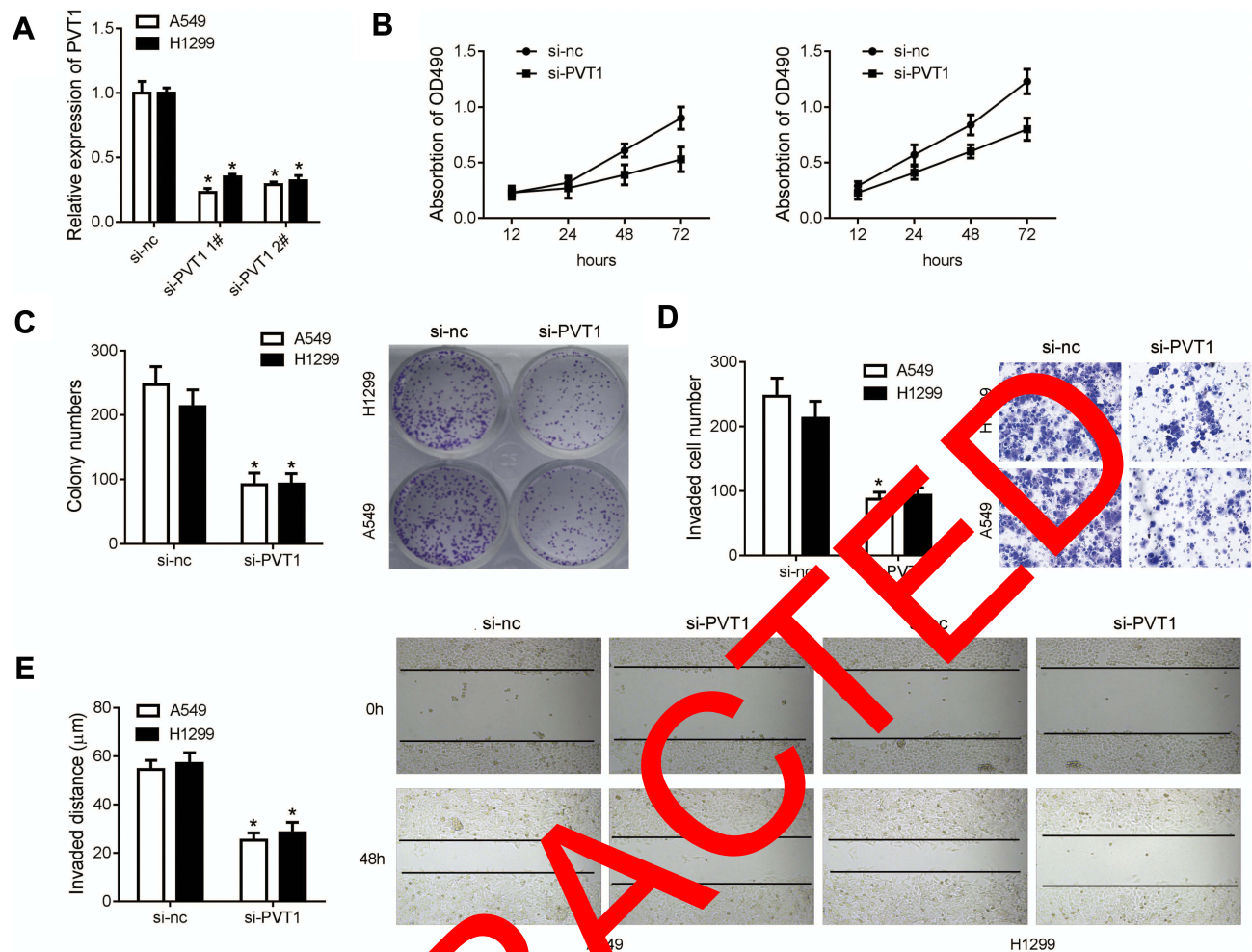


**Figure 3** PVT1 knock down inhibited the proliferation and migration of NSCLC cell lines in vitro. **(A)** Transfection effect of si-PVT1 was detected by qRT-PCR assay. **(B)** Proliferation ability of each group was measured by CCK-8 assay and **(C)** colony formation assay. **(D)** Migration ability of each group was detected by transwell assay and **(E)** wound healing assay. \* $p < 0.05$  vs si-NC group.

RAB34-wt, but no change was observed in RAB34-3'UTR-mut group (Figure 6B). The effect of miR-148 on expression of RAB34 was detected by Western blot and the result showed that miR-148-mimics reduced the protein expression of RAB34 (Figure 6C). Then, the correlation analysis showed that there was a significantly negative correlation between miR-148 and RAB34 (Figure 6D).

Through analyzing the profiles of NSCLC patient from Gene Expression Omnibus (GEO), we found that RAB34 was up-regulated in NSCLC tissues compared with normal lung tissues (Figure 6E). The expression of RAB34 in NSCLC tissues and cells was detected via qRT-PCR assay and the result indicated that RAB34 is significantly highly expressed in NSCLC tissues and cells compared with the corresponding control group (Figure 6F and G). The results of immunohistochemistry

experiments also showed that RAB34 is highly expressed in NSCLC tissues significantly (Figure 6J). Since the expression of miR-148 is negatively correlated with RAB34 and PVT1, we hypothesized that PVT1 positively regulates the expression of RAB34. The correlation analysis of the mRNA expression confirmed that RAB34 was positively correlated with PVT1 (Figure 6H). We performed Western blot assay to detect the effect of miR-148 and PVT1 on the protein expression of RAB34 in A549 and H1299 cells. Over-expression of PVT1 can increase the protein expression of RAB34, while over-expression of miR-148 can reverse this effect (Figure 6I). Then, we evaluated the expression of RAB34 in NSCLC and normal tissue using IHC. As Figure 6J revealed, expression level of RAB34 in NSCLC tumor tissues is much high than that in normal tissues.







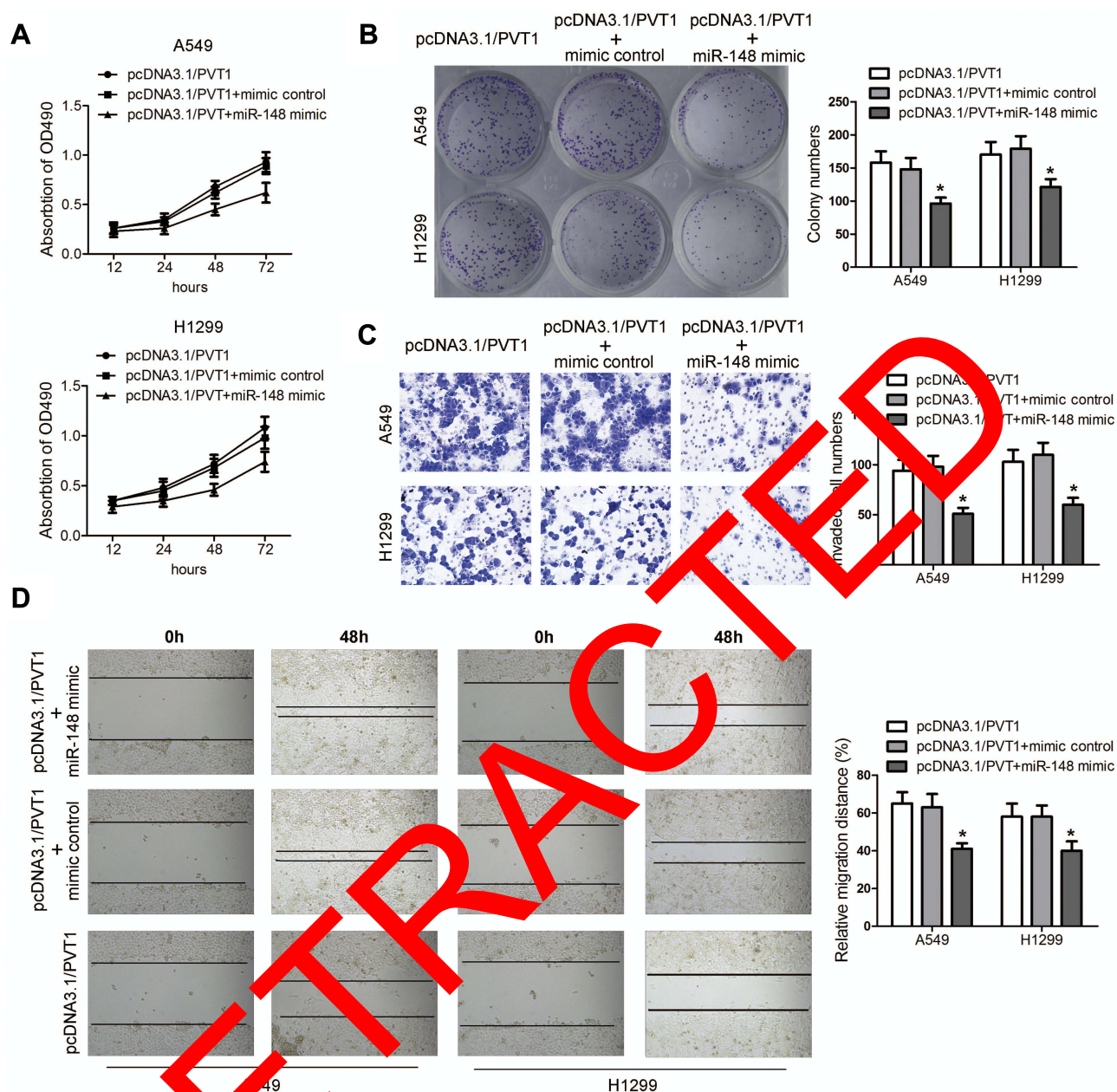


**Figure 5** MiR-148 inhibited the growth of PVT1 in vitro. Cells were transfected with PVT1, PVT1+mimic control or PVT1+miR-148 mimic. Proliferation ability of each group was measured by (A) CCK-8 assay and (B) colony formation assay. Migration ability of each group was detected by (C) transwell assay and (D) wound healing assay. \* $p < 0.05$  vs pcDNA3.1/PVT1+mimic control group.

(Figure 9A and B). At last, the tumors were removed and weighed. The mean tumor weight of RAB34 over-expressing group was significantly higher than that in the control group and the tumor weight of RAB34 down-regulating group was lower than that in the control group (Figure 9C).

## Discussion

NSCLC accounts for more than 80% of lung cancer which is the primary cause of cancer-related deaths worldwide.<sup>1,20</sup>

Although numerous treatments are available, the survival rates of NSCLC patients are still low.<sup>2,21</sup> Therefore, it is necessary to find potential therapeutic targets of NSCLC. In recent years, many studies have revealed that the expression of lncRNAs is aberrant in human cancer.<sup>22</sup> It has been reported that the expression of lncRNA PVT1 was up-regulated in NSCLC and promotes the tumorigenesis in NSCLC.<sup>23</sup> However, the underlying mechanism remains poorly understood. For instance, PVT1 is able to bind miR-497 and regulate the expression of its downstream gene LATS2.<sup>9,10</sup>

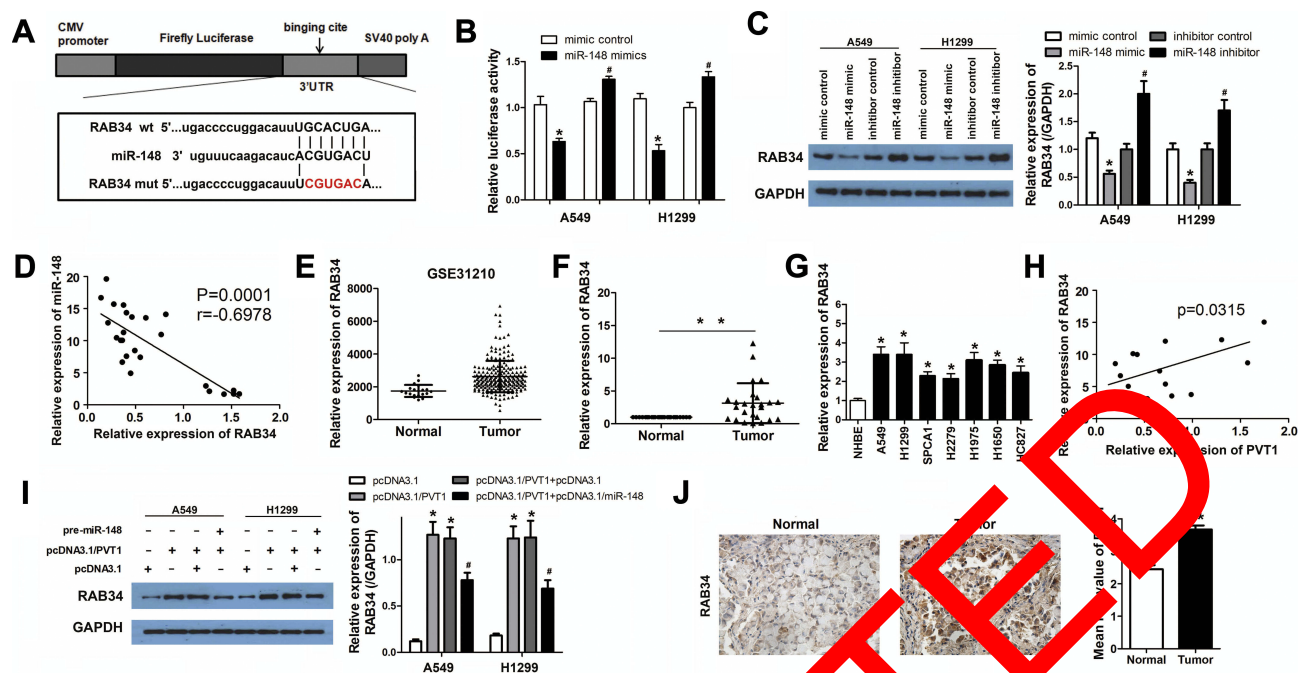


**Figure 6** RAB34 is a direct target of miR-148 in A549 and H1299 and RAB34 expression is up-regulated in NSCLC. (A) Schematic of the predicted binding sequences of miR-148 in the wild-type and mutant (in red) 3'UTR of RAB34. (B) The dual-luciferase assay was performed to prove the relationship between miR-148 and RAB34. (C) The protein expression of RAB34 in A549 and H1299 cells was tested by WB after the transfection of miR-148-mimics or miR-148-inhibitor. (D) The correlation analysis between the expression of RAB34 and the expression of miR-148 in NSCLC. (E) Relative expression of RAB34 in the profiles of NSCLC patient tissues from GEO. (F) RAB34 expression in 25 paired NSCLC tissues compared with normal tissues was detected by RT-PCR assay. (G) RAB34 expression was examined by qRT-PCR in NSCLC cell lines (A549, H1299, SPCA1, H2279, H1975, H1650, HC827) and human normal bronchial epithelial cells (NHBE). (H) The correlation analysis between the expression of PVT1 and the expression of RAB34 in NSCLC. (I) The effect of miR-148 and PVT1 on the expression of RAB34 was detected by Western blot. (J) The expression of RAB34 in NSCLC tissues and normal tissues was examined by immunohistochemical staining and the mean IOD value was calculated. \* $p < 0.05$  vs mimic control, pcDNA3.1, normal and MHBE groups, respectively, \*\* $p < 0.01$  vs normal group, # $p < 0.05$  vs inhibitor control group.

In this study, we aim to extend our knowledge about the molecular mechanism underlying the effect of PVT1. We found that the expression of lncRNA PVT1 was statistically higher in both NSCLC tissues and cells and demonstrated that PVT1 promoted the proliferation and migration of NSCLC cells, which is consistent with the previous studies. Then, we performed dual luciferase assay to reveal that miR-148 targeted PVT1 and was down-regulated in NSCLC tissues and cells. Previous studies have indicated that PVT1 targets miR-195 and miR-216b in NSCLC.<sup>12</sup> The binding sites of miR-195, miR-216b and miR-148 locate in the different region of PVT1 sequence.<sup>19</sup> To extend our understanding of the mechanism underlying the effect of PVT1, we chose miR-148 for the further research which has not been studied as the target of PVT1. The down-regulation of miR-148 was related to poor prognosis of NSCLC patients. MiR-148a, miR-148b and miR-152 which were the three members of the miR-148/152 family have been identified to have a low expression in NSCLC tissues and cells.<sup>24</sup> Moreover, the level of miR-148 in plasma samples of non-small cell lung cancer patients was also lower than that of normal patients.

These findings indicated the potential critical effect of miR-148 in the progression of NSCLC. We determined that miR-148 targeted PVT1 and was capable of reversing the function of PVT1 which verified our speculation.

It is well known that ceRNA is the main mechanism involved in the function of lncRNAs.<sup>25,26</sup> In this way, lncRNAs competing with the other genes to bind with miRs, thus spared the negative regulation of miRs on their target genes. We also tried to find the ceRNA of PVT1. The TargetScan website revealed that miR-148a, miR-148b, and miR-152 both bind to RAB34 and the binding sites are identical. RAB family proteins play a vital role in the initiation and progression of tumors.<sup>27</sup> Rab proteins regulate cancer cell migration and invasion through modulating surface protein internalization, degradation, and recycling.<sup>28,29</sup> RAB34 leads to poor prognosis in high-grade glioma patients<sup>18</sup> which was overexpressed in HCC and may become a biomarker and therapeutic target for HCC.<sup>30</sup> Previous results uncovered the role of Rab34 in migration and invasion of breast cancer cells and its involvement in cancer metastasis.<sup>15</sup> In spite of these findings, the function of RAB34 in NSCLC was unclear.



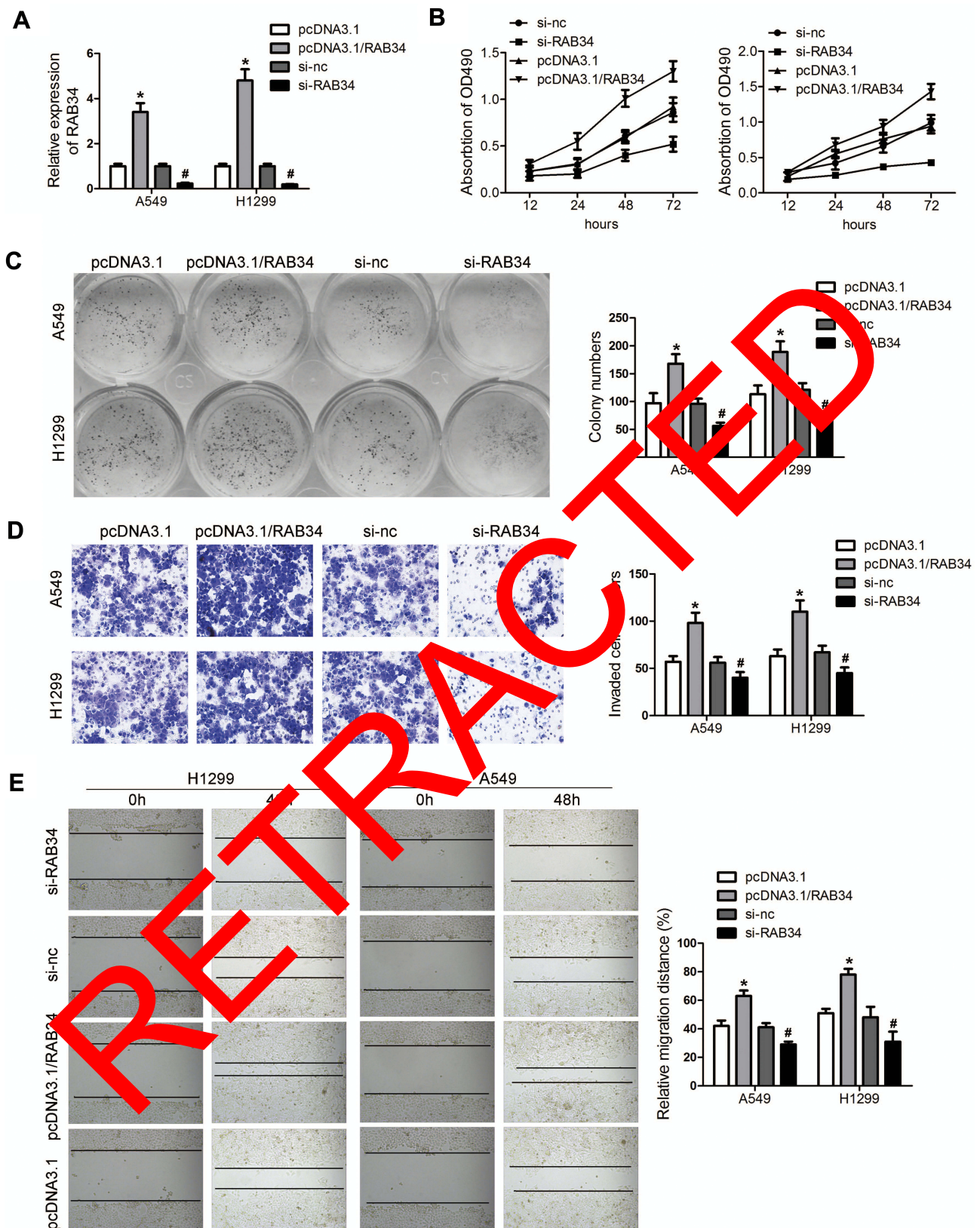


**Figure 7** RAB34 promotes the proliferation and migration of NSCLC cell lines in vitro. **(A)** The effect of over-expression and knockdown of PVT1 was detected by qRT-PCR assay. **(B)** Proliferation ability of each group was measured by CCK-8 assay and **(C)** colony formation assay. **(D)** Migration ability of each group was detected by transwell assay and **(E)** wound healing assay. \* $p < 0.05$  vs pcDNA3.1 group, # $p < 0.05$  vs si-NC control group.

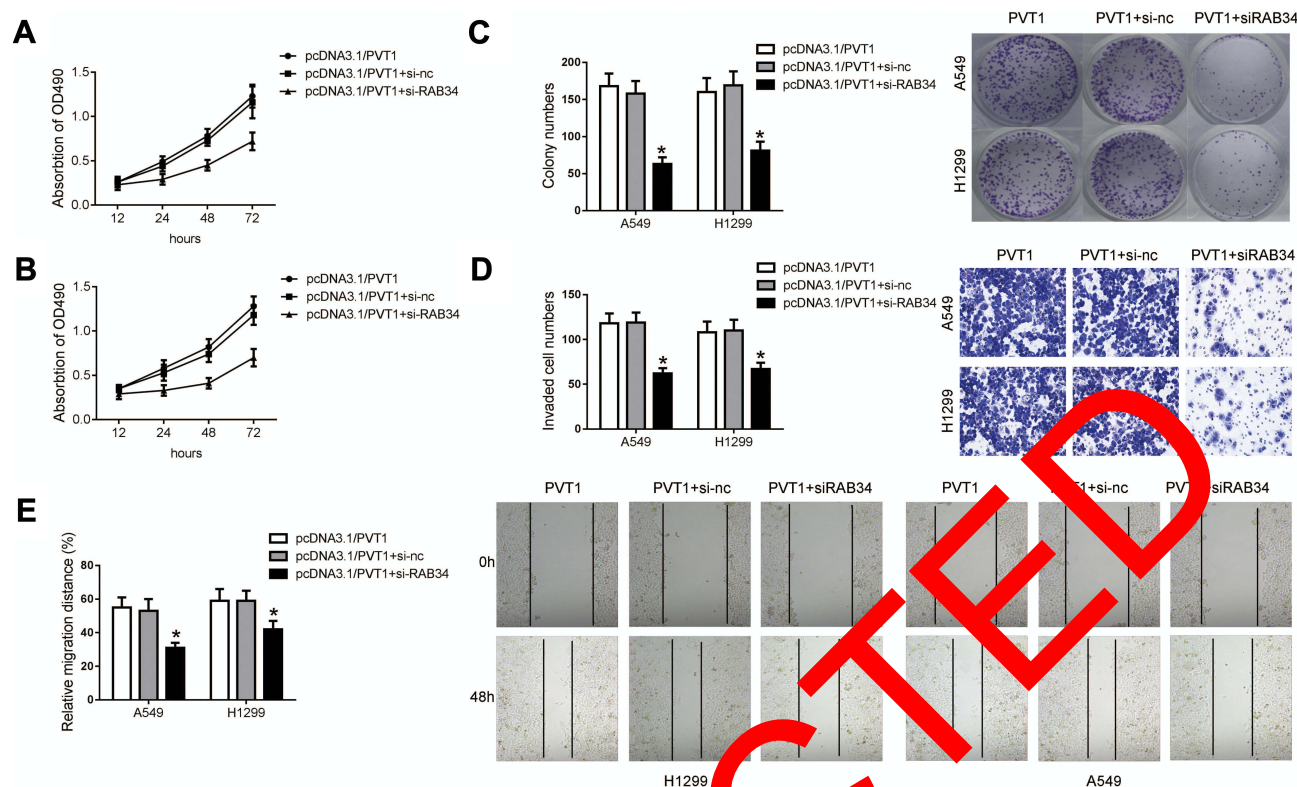


**Figure 8** RAB34 knock down reversed the effect of PVT1 in vitro. Cells were transfected with PVT1, PVT1+si-nc or PVT1+si-RAB34. Proliferation ability of each group was measured by (A, B) CCK-8 assay and (C) colony formation assay. Migration ability of each group was detected by (D) transwell assay and (E) wound healing assay. \* $p < 0.05$  vs PVT1+si-nc group.

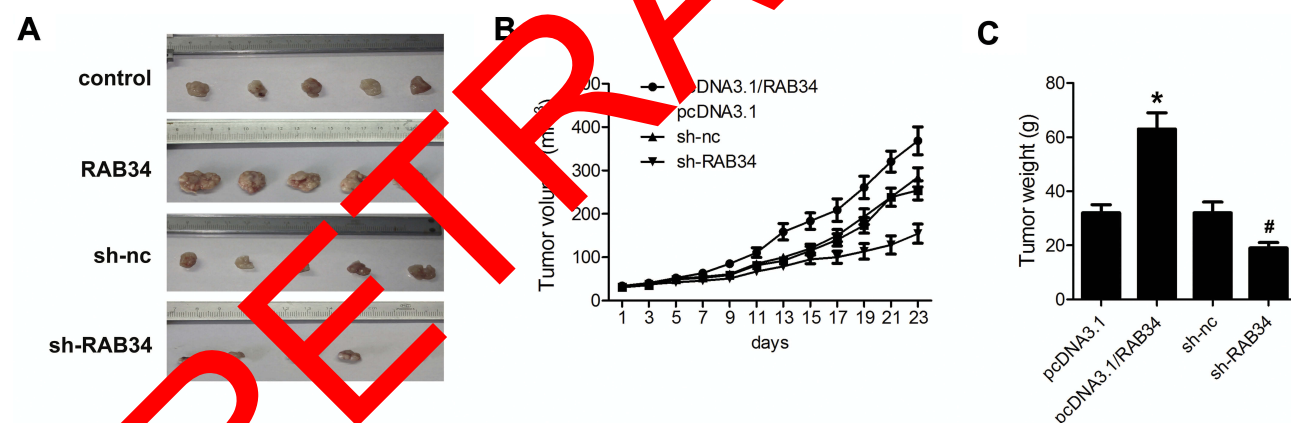


**Figure 9** RAB34 promotes tumor growth of NSCLC in vivo. (A) The picture of tumors. A549 cell lines that stably expressed pcDNA3.1-RAB34, sh-RAB34 or corresponding control were injected into the flanks of nude mice subcutaneously. (B) The mice were closely monitored for tumor growth and tumor volume was measured at the indicated times. (Tumor volume =  $1/2 \times (\text{width})^2 \times \text{length}$ ) (C) The weight of tumor in each group. \* $p < 0.05$  vs pcDNA3.1 group, # $p < 0.05$  vs sh-NC control group.

In our study, the expression of RAB34 was verified to be up-regulated in NSCLC tissues and cells and is positively regulated by PVT1, meantime, negatively regulated by miR-148. As PVT1 and miR-148 have been reported to have critical roles in NSCLC, while RAB34 has not been studied before. Accordingly, we investigated the effect of RAB34 in the progression of NSCLC. To elucidate the

effect of RAB34 on NSCLC, we over-expressed the RAB34 by transient transfection of pcDNA3.1-RAB34 vector and reduced the endogenous RAB34 by transient transfection of siRNA-RAB34 in NSCLC cells. The proliferation of cells was detected by CCK8 and clone formation assay. The migration of cells was detected by transwell and wound healing assay. The results showed



that RAB34 could promote cell proliferation and migration in A549 and H1299 cells. The nude mice xenograft assay further determined that RAB34 could promote tumor growth in vivo.

In conclusion, we demonstrated that PVT1 exerts its oncogenic role by regulating the miR-148/RAB34 signal axis. We firstly discovered the function of RAB34 in NSCLC. Our findings spread out understanding on the effect of PVT1, miR-148 along with RAB34. RAB may become a new biomarker and therapeutic target for NSCLC. In addition, the PVT1/miR-148/RAB34 may become an important signal in NSCLC. However, the rescue experiments of the RAB34 and miR-148 as well as RAB34 and PVT1 are required to further confirm the ceRNA mechanism between RAB34 and PVT1.

## Disclosure

The authors report no conflicts of interest in this work.

## References

- Jemal A, Bray F, Center MM, Ferlay J, Ward E, Forman D. Global cancer statistics. *CA Cancer J Clin*. 2011;61(2):69–90. doi:10.3322/caac.v61i2
- Cheng H, Perez-Soler R. Leptomeningeal metastases in non-small-cell lung cancer. *Lancet Oncol*. 2018;19(1):e43–e55. doi:10.1016/S1470-2045(17)30689-7
- Lorenzen JM, Thum T. Long noncoding RNAs in kidney and cardiovascular diseases. *Nat Rev Nephrol*. 2016;12(5):360–371. doi:10.1038/nrneph.2016.51
- Thum T, Condorelli G. Long noncoding RNAs and microRNAs in cardiovascular pathophysiology. *Circ Res*. 2015;113(4):e1–e12. doi:10.1161/CIRCRESAHA.116.303555
- Uchida S, Dimmeler S. Long noncoding RNAs in cardiovascular diseases. *Circ Res*. 2015;116(4):e1–e12. doi:10.1161/CIRCRESAHA.116.302521
- Greco CM, Condorelli G. Epigenetic modifications and noncoding RNAs in cardiac hypertrophy and failure. *Nat Rev Cardiol*. 2015;12(8):488–497. doi:10.1038/nrcard.2015.71
- Wang L, Ma L, Xu J, et al. Role of long non-coding RNA in drug resistance in non-small cell lung cancer. *Thorac Cancer*. 2018;9(7):761–770. doi:10.1111/tc.12188
- Cui D, Yu CH, Liu M, Xiao SQ, Zhang YF, Jiang WL. Long noncoding RNA PVT1 as a novel biomarker for diagnosis and prognosis of non-small cell lung cancer. *Tumour Biol*. 2016;37(3):4127–4134. doi:10.1007/s13277-015-4261-x
- Qin S, Zhao Y, Lim G, Lin H, Zhang X, Zhang X. Circular RNA PVT1 acts as a competing endogenous RNA for miR-497 in promoting non-small cell lung cancer progression. *Biomed Pharmacother*. 2019;111:244–250. doi:10.1016/j.biopha.2018.12.007
- Wan L, Sun M, Liu GJ, et al. Long noncoding RNA PVT1 promotes non-small cell lung cancer cell proliferation through epigenetically regulating LATS2 expression. *Mol Cancer Ther*. 2016;15(5):1082–1094. doi:10.1158/1535-7163.MCT-15-0707
- Wu D, Li Y, Zhang H, Hu X. Knockdown of lncRNA PVT1 enhances radiosensitivity in non-small cell lung cancer by sponging Mir-195. *Cell Physiol Biochem*. 2017;42(6):2453–2466. doi:10.1159/000480209
- Chen L, Han X, Hu Z, Chen L. The PVT1/miR-216b/Beclin-1 regulates cisplatin sensitivity of NSCLC cells via modulating autophagy and apoptosis. *Cancer Chemother Pharmacol*. 2019;83(5):921–931. doi:10.1007/s00280-019-03808-3
- Li L, Chen YY, Li SQ, Huang C, Qin YZ. Expression of miR-148/152 family as potential biomarkers in non-small-cell lung cancer. *Med Sci Monit*. 2015;21:1155–1161. doi:10.12659/MSM.892940
- Huang MX. Down-expression of circulating micro ribonucleic acid (miRNA)-148/152 family in plasma samples of non-small cell lung cancer patients. *J Cancer Res Ther*. 2016;12(2):671–675. doi:10.4103/0973-1482.150420
- Sun L, Xu X, Chen Y, et al. Rab34 regulates adhesion, migration, and invasion of breast cancer cells. *Oncogene*. 2018;37(27):3698–3714. doi:10.1038/s41388-018-0202-7
- Starling GP, Yip YY, Sanger A, Morton CL, Eden ER, Dodding MP. Folliculin directs the formation of a Rab34-Rab1 complex to control the nutrient-dependent dynamic distribution of lysosomes. *EMBO Rep*. 2016;17(6):823–841. doi:10.15252/embr.20151382
- Luo H, Zhang H, Zhang WZ, et al. Down-regulated miR-9 and miR-433 in human gastric carcinoma. *J Exp Clin Cancer Res*. 2009;28:82. doi:10.1186/1756-9966-28-82
- Wang HJ, Gao Y, Chen L, Li J, Jiang CL. RAB34 was a progression- and prognosis-associated marker in gliomas. *Tumour Biol*. 2015;36(3):1573–1578. doi:10.1007/s13277-014-2732-0
- Nagy A, Csizsar A, Menyhai Z, Györfi B. Validation of miRNA prognostic power in hepatocellular carcinoma using expression data of independent datasets. *Sci Rep*. 2018;8:9227. doi:10.1038/s41598-018-27521-y
- Yanaihara N, Caplen N, Bowman E, et al. Unique microRNA molecular profile in lung cancer diagnosis and prognosis. *Cancer Cell*. 2006;9(3):187–198. doi:10.1016/j.ccr.2006.01.025
- Bray F, Ferlay J, Soerjomataram I, et al. Global cancer statistics 2018: GLOBOCAN estimates of incidence and mortality worldwide for 36 cancers in 185 countries. 2014. *CA Cancer J Clin*. 2018;68(2):394–424. doi:10.3322/caac.21492
- Spizzo R, Almeida MI, Colombatti A, Calin GA. Long non-coding RNAs and cancer: a new frontier of translational research? *Oncogene*. 2012;31(43):4577–4587. doi:10.1038/onc.2011.621
- Yang YR, Zang SZ, Zhong CL, Li YX, Zhao SS, Feng XJ. Increased expression of the lncRNA PVT1 promotes tumorigenesis in non-small cell lung cancer. *Int J Clin Exp Pathol*. 2014;7(10):6929–6935.
- Cheng Z, Ma R, Tan W, Zhang L. MiR-152 suppresses the proliferation and invasion of NSCLC cells by inhibiting FGF2. *Exp Mol Med*. 2014;46:e112. doi:10.1038/emmm.2014.51
- Karret FA, Pandolfi PP. ceRNA cross-talk in cancer: when ce-bling rivalries go awry. *Cancer Discov*. 2013;3(10):1113–1121. doi:10.1158/2159-8290.CD-13-0202
- Tay Y, Rinn J, Pandolfi PP. The multilayered complexity of ceRNA crosstalk and competition. *Nature*. 2014;505(7483):344–352. doi:10.1038/nature12986
- Chia WJ, Tang BL. Emerging roles for Rab family GTPases in human cancer. *Biochim Biophys Acta*. 2009;1795(2):110–116. doi:10.1016/j.bbcan.2008.10.001
- Tang BL, Ng EL. Rabs and cancer cell motility. *Cell Motil Cytoskeleton*. 2009;66(7):365–370. doi:10.1002/cm.v66:7
- Porter N, Barbieri MA. The role of endocytic Rab GTPases in regulation of growth factor signaling and the migration and invasion of tumor cells. *Small GTPases*. 2015;6(3):135–144. doi:10.1080/21541248.2015.1050152
- Wu J, Lu Y, Qin A, Qiao Z, Jiang X. Overexpression of RAB34 correlates with poor prognosis and tumor progression in hepatocellular carcinoma. *Oncol Rep*. 2017;38(5):2967–2974. doi:10.3892/or.2017.5957

RETRACTED

OncoTargets and Therapy

Dovepress

### Publish your work in this journal

OncoTargets and Therapy is an international, peer-reviewed, open access journal focusing on the pathological basis of all cancers, potential targets for therapy and treatment protocols employed to improve the management of cancer patients. The journal also focuses on the impact of management programs and new therapeutic

agents and protocols on patient perspectives such as quality of life, adherence and satisfaction. The manuscript management system is completely online and includes a very quick and fair peer-review system, which is all easy to use. Visit <http://www.dovepress.com/testimonials.php> to read real quotes from published authors.

Submit your manuscript here: <https://www.dovepress.com/oncotargets-and-therapy-journal>